FEASIBILITY ANALYSIS OF A COMBINED CHEMICAL LOOPING COMBUSTION AND RENEWABLE-ENERGY-BASED METHANE PRODUCTION SYSTEM FOR CO_2 CAPTURE AND UTILIZATION

by

Piero BARESCHINO[a*], Erasmo MANCUSI[a], Francesco PEPE[a], Massimo URCIUOLO[b], and Antonio COPPOLA[b]

[a] Department of Engineering, University of Sannio, Benevento, Italy
[b] Combustion Research Institute, Nation Council of Researches, Napoli, Italy

Original scientific paper
https://doi.org/10.2298/TSCI200328281B

Power-to-methane represents an innovative approach to convert electrical into chemical energy. Such a technology could actually be successful only when the coupling of a cost-effective source of electrical energy and a pure CO_2 stream is carried out. Under this perspective, this paper numerically investigates an innovative process layout that integrates a fluidized beds chemical looping system for the combustion of solid fuels and a renewable-based power-to-methane system. Process performances were evaluated by considering a coal and three sewage sludge, differing in water content, as fuels, CuO supported on zirconia as oxygen carrier, hydrogen production via water electrolysis, and Ni supported on alumina as methanation catalyst. Autothermal feasibility of the process was assessed by considering that part of the produced CH_4 can eventually be burned to dry high-moisture-content fuels. Finally, by considering that only electric energy from renewable sources is used, the capability of the proposed process to be used as an energy storage system was evaluated.

Keywords: *thermal power plants, chemical looping combustion, CO_2 capture and utilization, methanation, numerical model*

Introduction

The reduction of CO_2 emissions directly related to energy production is a challenge that our societies have to tackle [1]. In this light, electricity production from renewable sources significantly increases over the last decade (*e.g.* in the EU it grows from 127 up to 476 TWh per year). Integrating such large amounts of renewable energies into existing energy grid poses some technological difficulties as a consequence of both their intrinsic uncertainty, and the inherent structure of the electric transmission grid [1]. Storing large amounts of electrical energy from renewable sources will help to mitigate such problems and to improve further diffusion of renewable energies. The H_2 production using electrolysis driven by excess or unbalancing electricity, power-to-gas (PtG), has been proposed as a viable option for long-term energy storage. The main idea of the PtG process is to convert electrical into chemical energy, allowing for more longstanding energy storage with respect to batteries [2].

*Corresponding author, e-mail: pbaresch@unisannio.it

In an energy system with large shares of renewable energy, PtG provides one of the most promising options to get to large-scale and flexible energy storage. The PtG can add balancing to the electricity grid, and provide the back-up capacity needed to secure supply for the end-users, and stabilize the market prices. To overcome the issues connected to H_2 storage, additional synthesis steps from H_2 to more stable fuels and/or chemicals have been proposed in [1]. Among synthesis fuels, CH_4 offers the possibility to store large amounts of energy from renewable sources for long time scales in an already existing storage system, the natural gas grid; moreover, it can be directly used in most of the endothermic engines and all other well-established natural gas facilities. Power-to-methane (PtM) involves three main processes: water electrolysis, CO_2 production or capture ant methanation, *i.e.* reaction between H_2 and CO_2 to produce CH_4. Differently from H_2 the CH_4 can be injected into the existing gas distribution grid or used as a motor fuel, attained that residual percentage of H_2 is lower than a given value. Consequently, PtM is quite complex, given the large number of units required and therefore suffer some drawbacks mainly related to low conversion efficiency and high operating costs [2]. In the following the state of the art of the main processes that compose the PtM is reported.

The PtM requires a carbon stream, thus being a natural candidate for carbon utilization after its capture. Indeed, one of the advantages of carbon capture utilization (CCU) over carbon capture sequestration (CCS) is that utilisation of CO_2 is normally a profitable activity as products can be sold such as chemicals and fuels [3]. Even though the conversion of CO_2 to various products is energy-intensive, owing to its thermodynamic stability, the potential for providing a secure supply of chemicals and fuels, along with the escalating fossil-fuel prices, could become a powerful driver for CCU [3].

Among carbon capture techniques, Chemical-looping-based CCS systems are under the spotlight as more efficient and cost-effective techniques than the current commercial capture technologies. Chemical looping are a set of technologies based on the cyclic exposition of solid metal oxide – identified as oxygen carrier (OC) – to two different reactive environments (*i.e.* two different reactors connected in a loop or two different streams alternatively fed to the same reactor *e.g.* [4]) so to selectively transport a chemical such as oxygen or CO_2 between otherwise uncoupled devices/environments [5]. Among them, chemical looping combustion with oxygen uncoupling (CLOU) is a very promising technology for solid fuels combustion with inherent CO_2 sequestration [6].

The CLOU concept is based on two cyclic steps: during the first one, the OC is reduced releasing gaseous oxygen for fuel oxidation (fuel reactor – FR), while in the second step (air reactor) the reduced OC is re-oxidized by air. Accordingly, direct contact between the fuel and atmospheric oxygen is avoided. The fuel and air reactors are most typically arranged as dual interconnected fluidized bed reactors, an arrangement that enables continuous recirculation of the catalyst between the two reactors while preventing gas leakage from one reactor to the other [7].

As previously discussed, water electrolysis can be used to produce H_2 taking advantage of the excess electrical energy. Water electrolysis is a well understood technology. Thereby, developments in fuel cell technology also helped to improve water electrolysis technologies. Three different electrolysis technologies are of interest for PtG process chains: alkaline electrolysis (AEL), polymer electrolyte membranes (PEM), and solid oxide electrolysis [8]. The AEL represent a mature technology and therefore, on the one hand, it has low installation costs, a good lifetime, and is available for large plant sizes. On the other hand, high maintenance costs are required (the system is highly corrosive) and, over the transient operation, reduction up

to 20% of nominal load is possible. On the contrary, PEM is recently emerging as substitutes to AEL since no corrosive substances are present, high power densities and high operating pressure, > 100 bar. can be reached, and can be operated dynamically.

Several reactor concepts have been proposed and investigated in [9] to carry out methanation reaction, ranging from multiple adiabatic layers fixed beds with inter-cooling and optional product recycle (*e.g.* TREMP [10] or Lurgi methanation [10]) to fluidized bed reactors (*e.g.* COMFLUX methanation [10]), with the aim of controlling the temperature rise associated to the highly exothermic Sabatier reaction so to avoid catalyst sintering while approaching the best thermodynamic condition for the process [9].

In this work, an innovative process layout to promote the integration among the chemical looping combustion of solid fuels, H_2 from renewable resources, and carbon methanation is numerically investigated. The performances of the system were evaluated by considering a coal and a sludge as fuels and CuO supported on zirconia as OC. A complex kinetic scheme comprising both gas-solid heterogeneous reactions taking place in the fluidized beds, involving both carbon and OC, and gas-phase homogeneous reactions occurring in the freeboard of FR was considered. The methanation unit was modelled developing a thermodynamic calculation method based on minimization of the free Gibbs energy [11]. The performance of the system was evaluated by considering that the CO_2 stream coming from the t-FR reacts with a pure H_2 stream from the electrolysis cell (EC) over NiO supported on alumina catalyst. The number of EC to be stacked in the array was evaluated by considering that a constant H_2 production able to convert the whole CO_2 stream produced by the CLC process should be attained. Moreover, by considering that only energy from renewable sources (such as photovoltaic panels or wind turbines) was fed to the EC, it was assessed the capability of the proposed process to be used as an energy storage system. At the best of authors' knowledge, there is no previous work in literature proposing the same configuration.

Mathematical model

Figure 1 reports the conceptual scheme of the proposed layout with details on the reactive pathways and the outlet and the inlet material streams. Three main units can be identified, namely the hydrogen production system (HPU), the fluidized beds chemical looping system for the combustion of solid fuels (CLOU), and the methanation reactor (MR). Fuel is fed to CLOU system (red dashed box in fig. 1). This latter is equipped with a two-stage FR, a riser used as air reactor, a cyclone, a L-valve return leg, and a loop-seal. In the first stage of the t-FR, where fuel and fresh OC from the air reactor enter, the solid fuel combustion took place. Volatile combustion occurs mainly in the second stage, where the partly reduced OC is present. An internal riser connects the two stages, thus allowing the solids to move from the first stage to the other. Solids from the second stage go through the loop-seal into the air reactor where the oxidation capability of the OC is restored. A cyclone collects the regenerated OC that is sent through the L-valve to the first stage of the t-FR. At the exit of the second stage, water and fines were separated from flue gas. A stream of CO_2 and H_2O leaves the FR. Water is separated by condensation and a pure stream of CO_2 is consequently produced. This latter is partly conveyed to the methanation unit (blue dashed box in fig. 1) to react with a H_2 stream coming from the EC array of the HPU (green dashed box in fig. 1), while the remnant is recycled to the t-FR. The HPU is fed by water and electrical energy considered to be produced only by renewable sources.

In the following, the mathematical models and the hypotheses made to describe the three units of the PtM process are reported.

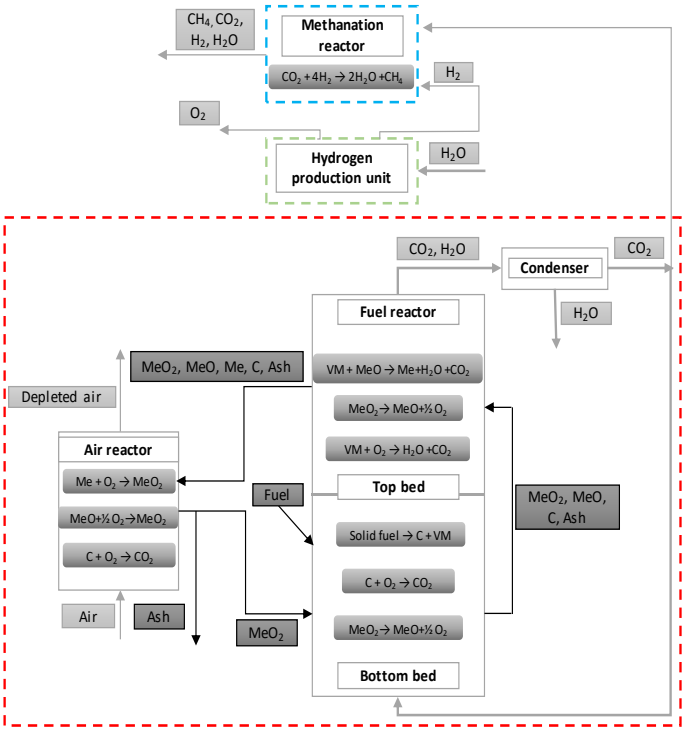

Figure 1. Conceptual scheme of the proposed process

Multiple interconnected fluidized bed

The model is based on the following hypothesis: steady-state; the dense zone of FR is well stirred with respect to both gas and solid species; the freeboard of FR conforms to plug flow; if air reactor works in the diluted regime, it is well-stirred respect to both gas and solid species, instead, if air reactor works in the dense regime it conforms to plug flow; conversion is uniform throughout the solid particles; steam and dry-reforming are negligible in the freeboard, in which only water gas shift reaction is taken into account; FR is isothermal; air reactor is adiabatic; conversion is uniform throughout the solid particles.

The gas-solid heterogeneous reactions taking place in the fluidized beds and the gas-phase homogeneous reactions occurring in the freeboard of FR implemented in the model were reported in tab. 1.

Table 1 Reactive scheme

r_1	$C+CO_2 \rightarrow 2CO$	r_8	$H_2+½O_2 \rightarrow H_2O$
r_2	$CuO+½CO \rightarrow ½Cu_2O+½CO_2$	r_9	$CuO+½H_2 \rightarrow ½Cu_2O+½H_2O$
r_3	$Cu_2O+CO \rightarrow 2Cu+CO_2$	r_{10}	$Cu_2O+H_2 \rightarrow 2Cu+H_2O$
r_4	$CuO \rightarrow ½Cu_2O+¼O_2$	r_{11}	$CuO+¼CH_4 \rightarrow Cu+¼CO_2+½H_2O$
r_5	$CO+½O_2 \rightarrow CO_2$	r_{12}	$CH_4+2O_2 \rightarrow CO_2+2H_2O$
r_6	$C+O_2 \rightarrow CO_2$	r_{13}	$Cu+½O_2 \rightarrow CuO$
r_7	$C+H_2O \rightarrow CO+H_2$	r_{14}	$Cu_2O+½O_2 \rightarrow 2CuO$

Reactions r_1-r_{12} were considered to occur in the FR, whereas reactions r_6, r_{13}, and r_{14} were referred to the air reactor. The whole set of heterogeneous and homogeneous reactions could be classified into three different categories: reactions involving carbon (r_1, r_6, r_7), reactions involving the OC (r_2-r_4, r_9-r_{11}, r_{13}, r_{14}), and reactions of the volatiles (r_5, r_8, r_{12}). More details on the adopted reaction kinetics and its validation can be found in [7].

Model equations consist of mass and energy balances on reagents and products. Mass balance equations, specialized to model the dense phase for both the bottom and the top bed, were referred or to single elements (*i.e.* C, H, O, Cu) or to specific compounds (*i.e.* CO_2, char, CH_4, H_2O) assuming the following general form:

$$\sum \dot{n}_i^{\text{in}} - \sum \dot{n}_i^{\text{out}} + \sum\left(\alpha_{i,j} r_j\right) = 0 \tag{1}$$

The complete set of equations is reported in tab. 2.

Table 2. Mass balance equations for the dense zone (bottom and top bed) in the FR

Element or compound	Equation
Atomic C	$\dot{n}_{\text{C}}^{\text{in}} + \dot{n}_{\text{CO}_2}^{\text{in}} + \dot{n}_{\text{CO}}^{\text{in}} + \dot{n}_{\text{CH}_4}^{\text{in}} - \dot{n}_{\text{C}}^{\text{out}} - \dot{n}_{\text{gas}}^{\text{out}} y_{\text{CO}_2}^{\text{out}} - \dot{n}_{\text{gas}}^{\text{out}} y_{\text{CO}}^{\text{out}} - \dot{n}_{\text{gas}}^{\text{out}} y_{\text{CH}_4}^{\text{out}} = 0$
Atomic Cu	$\dot{n}_{\text{CuO}}^{\text{in}} + 2\dot{n}_{\text{Cu}_2\text{O}}^{\text{in}} + \dot{n}_{\text{Cu}}^{\text{in}} - \dot{n}_{\text{CuO}}^{\text{out}} - 2\dot{n}_{\text{Cu}_2\text{O}}^{\text{out}} - \dot{n}_{\text{Cu}}^{\text{out}} = 0$
Atomic H_2	$\dot{n}_{\text{H}_2\text{O}}^{\text{in}} + \dot{n}_{\text{H}_2}^{\text{in}} + 2\dot{n}_{\text{CH}_4}^{\text{in}} - \dot{n}_{\text{gas}}^{\text{out}} y_{\text{H}_2\text{O}}^{\text{out}} - \dot{n}_{\text{gas}}^{\text{out}} y_{\text{H}_2}^{\text{out}} - 2\dot{n}_{\text{gas}}^{\text{out}} y_{\text{CH}_4}^{\text{out}} = 0$
Atomic O_2	$\dot{n}_{\text{CuO}}^{\text{in}} + \dot{n}_{\text{Cu}_2\text{O}}^{\text{in}} + 2\dot{n}_{\text{CO}_2}^{\text{in}} + \dot{n}_{\text{CO}}^{\text{in}} + 2\dot{n}_{\text{O}_2}^{\text{in}} + \dot{n}_{\text{H}_2\text{O}}^{\text{in}} - \dot{n}_{\text{CuO}}^{\text{out}} - \dot{n}_{\text{Cu}_2\text{O}}^{\text{out}} - 2\dot{n}_{\text{gas}}^{\text{out}} y_{\text{O}_2}^{\text{out}} - 2\dot{n}_{\text{gas}}^{\text{out}} y_{\text{CO}_2}^{\text{out}} - \dot{n}_{\text{gas}}^{\text{out}} y_{\text{H}_2\text{O}}^{\text{out}} - \dot{n}_{\text{gas}}^{\text{out}} y_{\text{CO}}^{\text{out}} = 0$
Copper oxide (II)	$\dot{n}_{\text{CuO}}^{\text{in}} - \dot{n}_{\text{CuO}}^{\text{out}} - W_{\text{CuO}}\left(r_2 + r_4 + r_9 + r_{11}\right) = 0$
Cu	$\dot{n}_{\text{Cu}}^{\text{in}} - \dot{n}_{\text{Cu}}^{\text{out}} + 2W_{\text{Cu}_2\text{O}}\left(r_3 + r_{10}\right) + W_{\text{CuO}} r_{11} = 0$
Carbon char	$\dot{n}_{\text{C}}^{\text{in}} - \dot{n}_{\text{C}}^{\text{out}} + W_{\text{C}}\left(-r_1 - r_6 - r_7\right) = 0$
Molecular O_2	$\dot{n}_{\text{O}_2}^{\text{in}} - \dot{n}_{\text{gas}}^{\text{out}} y_{\text{O}_2}^{\text{out}} + \frac{1}{4} W_{\text{CuO}} r_4 - W_{\text{C}} r_6 - \frac{1}{2} V^{\text{D}}\left(r_5 + r_8\right) - 2V^{\text{D}} r_{12} = 0$
H_2O	$\dot{n}_{\text{H}_2\text{O}}^{\text{in}} - \dot{n}_{\text{gas}}^{\text{out}} y_{\text{H}_2\text{O}}^{\text{out}} - W_{\text{C}} r_7 + V^{\text{D}} r_8 + \frac{1}{2} W_{\text{CuO}}\left(r_9 + r_{11}\right) + W_{\text{Cu}_2\text{O}} r_{10} + 2V^{\text{D}} r_{12} = 0$
CH_4	$\dot{n}_{\text{CH}_4}^{\text{in}} - \dot{n}_{\text{gas}}^{\text{out}} y_{\text{CH}_4}^{\text{out}} - \frac{1}{4} W_{\text{CuO}} r_{11} - V^{\text{D}} r_{12} = 0$
Gaseous species	$1 - y_{\text{CO}_2}^{\text{out}} - y_{\text{CO}}^{\text{out}} - y_{\text{O}_2}^{\text{out}} - y_{\text{H}_2\text{O}}^{\text{out}} - y_{\text{CH}_4}^{\text{out}} = 0$

To complete the set of equations reported in tab. 2 according to the main assumptions previously described: in the freeboard of the bottom and the top bed, only homogeneous reactions of the gaseous compounds were taken into account. Thus mass balances have been expressed by means of differential equations (see tab. 3) as follows:

$$\frac{1}{S_{\text{FB}}} \frac{\text{d}\dot{n}_i^{\text{FB}}}{\text{d}h} = \sum\left(\alpha_{i,j} r_j\right) \tag{2}$$

Energy balance equations, tab. 4, used to calculate the thermal power needed to ensure isothermal reactor operation at the pre-set temperature, were written as:

$$\sum \dot{n}_i^{\text{in}} c_{p,i} \left(T^\circ - T_i^{\text{in}}\right) + \sum \dot{n}_i^{\text{out}} c_{p,i} \left(T_i^{\text{out}} - T^\circ\right) + \sum \left(-H_{r_j}^\circ\right) r_j + \dot{Q} = 0 \tag{3}$$

Table 3. Differential equations for mass balance in the freeboard of the FR

CO_2	$\frac{1}{S_{\text{FB}}} \frac{\text{d}\dot{n}_{\text{CO}_2}^{\text{FB}}}{\text{d}h} = r_5 + r_{12}$	O_2	$\frac{1}{S_{\text{FB}}} \frac{\text{d}\dot{n}_{\text{O}_2}^{\text{FB}}}{\text{d}h} = -\frac{1}{2} r_5 - \frac{1}{2} r_8 - 2r_{12}$
CO	$\frac{1}{S_{\text{FB}}} \frac{\text{d}\dot{n}_{\text{CO}}^{\text{FB}}}{\text{d}h} = -r_5$	H_2O	$\frac{1}{S_{\text{FB}}} \frac{\text{d}\dot{n}_{\text{H}_2\text{O}}^{\text{FB}}}{\text{d}h} = r_8 + 2r_{12}$
H_2	$\frac{1}{S_{\text{FB}}} \frac{\text{d}\dot{n}_{\text{H}_2}^{\text{FB}}}{\text{d}h} = -r_8$	CH_4	$\frac{1}{S_{\text{FB}}} \frac{\text{d}\dot{n}_{\text{CH}_4}^{\text{FB}}}{\text{d}h} = -r_{12}$
Total gas moles	$\frac{1}{S_{\text{FB}}} \frac{\text{d}\dot{n}_{\text{gas}}^{\text{FB}}}{\text{d}h} = -\frac{1}{2} r_5 - \frac{1}{2} r_8$		

Table 4. Energy balance equations for the fuel and air reactor

Fuel reactor energy balance	$(\dot{n}_{\text{S}}^{\text{in}} c_{p,\text{S}} + \dot{n}_{\text{CuO}}^{\text{in}} c_{p,\text{CuO}})(T^\circ - T^{\text{AR}}) + \dot{n}_{\text{gas}}^{\text{in}} (y_{\text{CO}_2}^{\text{in}} c_{p,\text{CO}_2} + y_{\text{H}_2\text{O}}^{\text{in}} c_{p,\text{H}_2\text{O}})(T^\circ - T_{\text{gas}}^{\text{in}}) +$ $+(\dot{n}_{\text{C}}^{\text{in}} c_{p,\text{C}} + \dot{n}_{V,\text{H}_2\text{O}}^{\text{in}} c_{p,\text{H}_2\text{O(l)}} + \dot{n}_{V,\text{CO}}^{\text{in}} c_{p,\text{CO}} + \dot{n}_{V,\text{H}_2}^{\text{in}} c_{p,\text{H}_2} + \dot{n}_{V,\text{CH}_4}^{\text{in}} c_{p,\text{CH}_4} +$ $+\dot{n}_{\text{Ash}}^{\text{in}} c_{p,\text{Ash}}) \left(T^\circ - T_{\text{Fuel}}^{\text{in}}\right) + \dot{n}_{V,\text{H}_2\text{O}}^{\text{in}} (-\lambda_{\text{Vap,H}_2\text{O}}) + [\dot{n}_{\text{S}}^{\text{out}} c_{p,\text{S}} + \dot{n}_{\text{CuO}}^{\text{out}} c_{p,\text{CuO}} + \dot{n}_{\text{Cu}_2\text{O}}^{\text{out}} c_{p,\text{Cu}_2\text{O}} +$ $+\dot{n}_{\text{Cu}}^{\text{out}} c_{p,\text{Cu}} + \dot{n}_{\text{C}}^{\text{out}} c_{p,\text{C}} + \dot{n}_{\text{Ash}}^{\text{out}} c_{p,\text{Ash}} + \dot{n}_{\text{gas}}^{\text{out}} (y_{\text{CO}_2}^{\text{out}} c_{\text{CO}_2} + y_{\text{CO}}^{\text{out}} c_{\text{CO}} + y_{\text{O}_2}^{\text{out}} c_{\text{O}_2} + y_{\text{H}_2\text{O}}^{\text{out}} c_{\text{H}_2\text{O}} +$ $+y_{\text{H}_2}^{\text{out}} c_{\text{H}_2} + y_{\text{CH}_4}^{\text{out}} c_{\text{CH}_4})](T^{\text{FR}} - T^\circ) + W_{\text{C}} (-\Delta H_{r_1}^\circ) r_1 + W_{\text{CuO}} (-\Delta H_{r_2}^\circ) r_2 + W_{\text{Cu}_2\text{O}} (-\Delta H_{r_3}^\circ) r_3 +$ $+W_{\text{CuO}} (-\Delta H_{r_4}^\circ) r_4 + V^{\text{FR}} (-\Delta H_{r_5}^\circ) r_5 + W_{\text{C}} (-\Delta H_{r_6}^\circ) r_6 + W_{\text{C}} (-\Delta H_{r_7}^\circ) r_7 + V^{\text{FR}} (-\Delta H_{r_8}^\circ) r_8 +$ $+W_{\text{CuO}} (-\Delta H_{r_9}^\circ) r_9 + W_{\text{Cu}_2\text{O}} (-\Delta H_{r_{10}}^\circ) r_{10} + W_{\text{CuO}} (-\Delta H_{r_{11}}^\circ) r_{11} + V^{\text{FR}} (-\Delta H_{r_{12}}^\circ) r_{12} + \dot{Q}^{\text{FR}} = 0$
Air reactor energy balance	$(\dot{n}_{\text{S}}^{\text{in}} c_{p,\text{S}} + \dot{n}_{\text{CuO}}^{\text{in}} c_{p,\text{CuO}} + \dot{n}_{\text{Cu}_2\text{O}}^{\text{in}} c_{p,\text{Cu}_2\text{O}} + \dot{n}_{\text{Cu}}^{\text{in}} c_{p,\text{Cu}} + \dot{n}_{\text{C}}^{\text{in}} c_{p,\text{C}} + \dot{n}_{\text{Ash}}^{\text{in}} c_{p,\text{Ash}})(T^\circ - T^{\text{FR}}) +$ $+\dot{n}_{\text{air}}^{\text{in}} [y_{\text{O}_2}^{\text{out}} c_{\text{O}_2} + y_{\text{N}_2}^{\text{out}} c_{\text{N}_2}](T^\circ - T^{\text{air}}) + [\dot{n}_{\text{S}}^{\text{out}} c_{p,\text{S}} + \dot{n}_{\text{CO}}^{\text{out}} c_{p,\text{CuO}} + \dot{n}_{\text{Ash}}^{\text{out}} c_{p,\text{Ash}} + \dot{n}_{\text{gas}}^{\text{out}} (y_{\text{CO}_2}^{\text{out}} c_{\text{CO}_2} +$ $+y_{\text{O}_2}^{\text{out}} c_{\text{O}_2} + y_{\text{N}_2}^{\text{out}} c_{\text{N}_2})](T^{\text{AR}} - T^\circ) + \dot{n}_{\text{C}}^{\text{in}} (-\Delta H_{r_6}^\circ) + \dot{n}_{\text{Cu}}^{\text{in}} (-\Delta H_{r_{13}}^\circ) + \dot{n}_{\text{Cu}_2\text{O}}^{\text{in}} (-\Delta H_{r_{14}}^\circ) + \dot{Q}^{\text{AR}} = 0$

The numerical model was solved using the commercial software package Comsol Muliphysics® and validated according to [5, 7, 12].

Methanation Unit

The methanation reactor has been modelled considering that CO_2 reacts with H_2 over Ni supported on alumina catalyst under equilibrium conditions and developing a thermodynamic calculation method based on the minimization of the free Gibbs energy [10]. Such a method does not rely on the actual reactor type, thus greatly reducing the computational effort, and is based on the principle that the system total Gibbs energy, accounting for condensed and non-reacting species too, reaches its minimum value at chemical equilibrium. Accordingly, if all the species, both reactants and products, in a reactive system are known, the concentration values at equilibrium can be evaluated by using a general mathematical technique even if the kinetic pathway is unknown. In the case of methanation processes, alt-

hough reactions pathway is well known, the mathematical problem of finding the equilibrium composition can be reformulated as the search for the minimum of the total Gibbs energy, neglecting the kinetic description of the process. The total Gibbs energy is given by:

$$\left(G^{\mathrm{t}}\right)_{T,P} = g\left(n_1, n_2, n_3, \ldots, n_{\mathrm{N}}\right) = \sum_{i=1}^{N} n_i G_i^{\circ} + \mathrm{R}T \sum_{i=1}^{N} \ln\left(\frac{f_i}{f_i^{\circ}}\right) \tag{4}$$

The problem is to find the set n_i which minimizes G^t for given values of pressure and temperature, subject to the constraints of the material balances. The material balance on each element k may be written assuming that the total number of atoms of each element is constant:

$$\sum_i n_i \upsilon_{i,k} = A_k \tag{5}$$

In eq. (5) A_k is the total number of atomic masses of the k^{th} element (C, H, O) in the system, as determined by the initial constitution of the system; $\upsilon_{i,k}$ is the number of atoms of the k^{th} element present in each molecule of chemical species i. The Gibbs energy for these species is calculated from the Gibbs-Helmholtz relation:

$$G = H - TS \tag{6}$$

where:

$$\begin{aligned} H &= H_{298} + \int_{298}^{T} c_p \mathrm{d}T \\ S &= S_{298} + \int_{298}^{T} \frac{c_p}{T} \mathrm{d}T \end{aligned} \tag{7}$$

The enthalpy at 298 K, H_{298}, is set to zero by convention. The entropy, S_{298}, is given by its absolute value, and the heat capacity at constant pressure, c_p, is calculated according to:

$$c_p = \mathrm{A} + \mathrm{B}T + \mathrm{C}T^2 + \mathrm{D}T^3 + \frac{\mathrm{E}}{T^2} \tag{8}$$

The coefficients of eq. (8) are from NIST Chemistry WebBook [13]. For solid Carbon a simplified formula for c_p has been used [14]:

$$c_p = \mathrm{A} + \mathrm{B}T - \frac{\mathrm{C}}{T^2} \tag{9}$$

The eq.(4) has to be written for each gaseous specie (i = CH_4, CO, CO_2, H_2, H_2O) and for solid carbon C. The minimum of this set of equations satisfying the constraint of conservation of atom, eq. (5), was found by exploiting the robust and popular function fmincon of MATLAB®.

Hydrogen production unit

Finally, the H_2 production unit was modelled as an array of high pressure polymer electrolyte membrane cells (HP-PEM). The number of HP-PEM to be arranged in the array was evaluated by considering that a constant H_2 production rate, capable of converting the whole CO_2 stream produced by the CLOU should be attained.

To assess the capability of the proposed process to be used as an energy storage system, the electric energy conversion efficiency, η_{ec}, defined as the ratio between the electric energy output and input of the system, was evaluated, according to:

$$\eta_{ec} = \frac{Q_{CH_4} LHV_{CH_4} CF \eta_e}{\text{Electric energy input}} \tag{10}$$

where Q_{CH_4} [Nm^3h^{-1}] is CH_4 volumetric flow-rate, LHV_{CH_4} [$kJkg^{-1}$] is CH_4 low heating value 50, CF [hy^{-1}] is the annual number of running hours, and η_e is thermal-to-electric conversion efficiency [7].

Materials and operating conditions

Properties of solid fuels, evaluated by means of proximate and ultimate analysis, carried out by LECO CHN 628, LECO CS 144 and LECO TG701, are reported in tab. 5.

Table 5. Properties of considered fuels

Type of fuel	Coal	Dewatered sludge	Semi-dried sludge	Dried sludge
Proximate analysis [–]				
Moisture	0.074	0.778	0.293	0.121
Volatiles	0.218	0.145	0.464	0.574
Fixed carbon	0.579	0.010	0.063	0.093
Ash	0.129	0.067	0.179	0.212
Ultimate analysis [–]				
C	0.727	0.496	0.523	0.519
H	0.048	0.077	0.072	0.074
N	0.013	0.073	0.086	0.088
S	0.066	0.007	0.016	0.013
O	0.146	0.346	0.303	0.306

For the CLOU unit, operating pressure was set at 1 bar, fuel and air reactor operating temperatures were set at 1173.15 K and 923.15 K, respectively. For the evaluation of the number of HP-PEM to be arranged in the array, data from commercially available units were considered [8]. Accordingly, a nominal H_2 production flowrate of 100 [Nm^3h^{-1}] and an electric energy efficiency equal to 46.6 kWh/kg_{H2} were taken into account. For the evaluation of the electric energy output of the system, η_e = 25% and CF = 6132.78 [h/y^{-1}] were assumed.

Results and discussion

On the basis of a 1 [kgh^{-1}] feed rate to the CLOU unit, tab. 6 reports, for the four considered fuels, the total thermal power, the CO_2 volumetric flow-rate, Q_{CO_2}, the required OC mass-flow-rate, and the fluidizing gas flow-rate to the air reactor. It is important to note that for the coal and the dried sludge, the model predicts that isothermal CLC can be carried out generating some thermal power. Instead, for dewatered and semi-dried sludge, isothermal CLC cannot be performed without the continuous input of external thermal power.

The fuel moisture content has also a strong effect on the CO_2 produced from the CLC system: as a matter of fact, the CO_2 produced with dewatered sludge is one order of magnitude lower than coal and this difference becomes less pronounced with the decreasing of moisture (semi-dried and dried sludges). Moreover, also the low carbon content of sludge (with respect to the coal) contributes to reducing the specific CO_2 production per mass of fed fuel. The low carbon content of sludges has a remarkable impact on the required OC mass-flow-rate, m_{oc}, despite dried sludge having a moisture content closer to coal, the required m_{oc} is halved with respect to the coal case, also implicating a decreasing of the fluidizing gas flow-rate to the Air reactor, Q_{air}.

Table 6. The MFB-CLC model outputs

	Coal	Dewatered sludge	Semi-dried sludge	Dried sludge
$Q_{T,H}$	−4.3	9.6	1.3	−1.4
Q_{CO_2}	3.7×10^{-4}	4.4×10^{-5}	1.5×10^{-4}	1.9×10^{-4}
m_{oc}	1.0×10^{-2}	1.1×10^{-3}	4.2×10^{-3}	5.2×10^{-3}
Q_{air}	3.7×10^{-6}	1.8×10^{-8}	1.5×10^{-6}	1.8×10^{-6}

The outgoing CO_2 stream from CLOU was fed to the methanation unit. The Sabatier methanation reaction is strongly exothermic and benefits from high pressures and low temperatures. Figure 2(a) reports, as a function of the operating temperature, the gas molar fractions at the output of the methanation unit when its operating pressure is set at 20 bar. The analysis of fig. 2(a) suggests that to achieve high CH_4 content while keeping H_2 concentration low, the temperature should be chosen as low as possible.

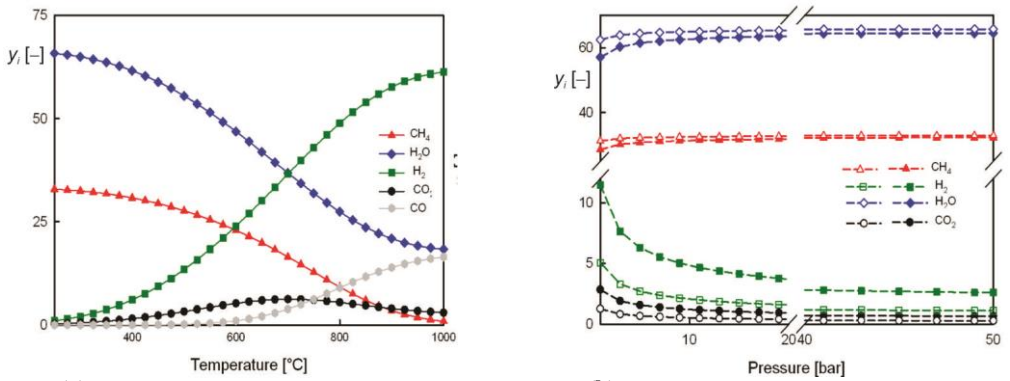

Figure 2. (a) Product fraction at the output of methanation unit as a function of operating temperature; H_2/CO_2=4, *P*=20 bar; (b) Gas outlet composition *vs.* pressure (bar) for two different temperatures. Filled symbols refer to 623 K empty symbols to 558 K.

Figure 2(b) reports, as a function of the operating pressure and parametric in the operating temperature, the gas molar fractions at the output of the methanation unit. It can be seen that: for any given temperature, maximum CH_4 concentration is reached before H_2 concentration approached its minimum as pressure increases; for any given pressure, an increase in the operating temperature lowers CH_4 concentration and increases H_2 one. Altogether, it can be inferred that: with respect to the choice of the operating temperature, above catalyst activation temperature the lower, the better; with respect to the choice of the operating pressure, a *threshold* pressure value exists for any given temperature beyond which any further pressure increase does not correspond to substantial variations in both H_2 and CH_4 concentrations. Furthermore, this has a beneficial effect to avoid carbon monoxide formation [15]. However, it should be noted that, depending on the type of catalyst, feed gas composition, and operating conditions, carbon deposition on the supported catalyst can occur (according to Boudouard reaction $2CO \leftrightarrow C + CO_2$); to avoid solid carbon formation, the temperature should be kept high or CO_2 and/or H_2O has to be added to the feed (*e.g.* [16]). Under the current assumption that H_2 and CO_2 are stoichiometrically fed to the methanation unit, no carbon deposition occurs. Accordingly, for any chosen operating pressure, the lower the operating temperature, the best in terms of CH_4 concentration.

The CO_2 flow-rate produced in CLOU, tab. 6, for each fed, tab. 5, has to be mixed with pure stream of H_2 in a stoichiometric ratio of H_2:CO_2 4:1 [9]. In tab. 7 reports the number of electrolytic cells, *Nc*, and the hydrogen, Q_{H_2}, and oxygen, Q_{O_2}, volumetric flow-rates. All the data refer to 1 [kgh^{-1}] of fuel fed.

Table 7. The HP-PEM model outputs

	Coal	Dewatered sludge	Semi-dried sludge	Dried sludge
Nc	5.3×10^{-2}	6.3×10^{-3}	2.1×10^{-2}	2.7×10^{-2}
Q_{H_2}	1.5×10^{-3}	1.7×10^{-4}	6.0×10^{-4}	7.6×10^{-4}
Q_{O_2}	7.4×10^{-4}	8.8×10^{-5}	3.0×10^{-4}	3.8×10^{-4}

Moreover, from fig. 2(a) and 2(b), it can be seen that, under any considered values of operating temperature and pressure, water concentration is higher than CH_4 one so drying of the methanation output stream is mandatory. After water removal, the concentration of CH_4 boosts together with the residual concentrations of both H_2 and CO_2. To improve process CH_4 yield, a second methanation unit could be placed in series with the first one. Table 8 reports, with respect to 1 [kgh^{-1}] of fuel fed, the carbon dioxide, Q_{CO_2}, hydrogen, and methane, Q_{CH_4}, volumetric flow-rates at the output of this second unit when the operating pressure is set at 20 [bar] and the operating temperature varies in a narrow interval above the catalyst activation one.

Table 8. Methanation units model outputs

	Coal		Dewatered sludge		Semi-dried sludge		Dried sludge	
T [K]	558	623	558	623	558	623	558	623
$Q_{CO_2}\times10^8$	7.40	9.77	0.88	1.16	3.00	3.96	3.80	5.02
$Q_{H_2}\times10^6$	6.96	9.77	0.83	1.16	2.82	3.96	3.57	5.02
$Q_{CH_4}\times10^4$	3.29	3.26	0.39	0.38	1.34	1.32	1.69	1.67

It should be noted here that, when the fuel CLC can be carried out isothermally (*i.e.* when the total thermal power is negative), the CH_4 volumetric flow-rate reported in tab. 8 is actually available to be stored or injected into a grid distribution system. On the contrary, in the attempt to achieve isothermal CLC, it could be partly or fully burned to feed the required external thermal power. Assuming that a heat recovery efficiency, η_{th}, of about 0.7 can be achieved by CH_4 burning, the amount of produced CH_4 to be burned, $Q_{CH4,b}$, can be calculated according to:

$$Q_{CH_4,b} = \frac{\dot{Q}_{TH}}{LHV_{CH_4}\eta_{th}} \tag{11}$$

This, in turns, makes semi-dried sludge isothermal CLC possible by burning around 40% of the produced CH_4 while, even burning the whole produced CH_4, the same cannot be for the dewatered sludge. The electric energy conversion efficiency evaluated for the fuels suitable to be used in the proposed process. A mean value of 13% has been assessed for η_{ec} regardless of both fuel type and methanation unit operating temperature. This value is consistent with those reported in the literature for chemical energy storage systems and, as such, lower than that of electrical storage processes. However, it is important to underline here that a comparison between electrical and chemical storage systems cannot rely on measuring up η_{ec} only, neglecting that for long-term energy storage chemicals systems are by far more efficient than electrical ones.

Conclusions

In this work, an innovative process layout to promote the integration among the CLC of solid fuels, solar H_2, and carbon methanation is numerically investigated. The performances of the CLC system were evaluated by considering a coal and sludges with different moisture content as fuels and CuO supported on zirconia as OC. The HPU was modelled by considering that a constant H_2 production able to convert the whole carbon stream produced by the CLC process should be attained. The performance of the HPU system was evaluated by considering data from commercially available units. The performance of the methanation system was evaluated by considering that the carbon stream coming from the t-FR reacts with a pure H_2 stream from the HPU over Ni supported on alumina catalyst. Net power production with reduced or near-zero CO_2 emissions can be attained, even when relatively high-moisture/ash-content fuels were fed to the system, by burning some of the produced CH_4. Only when very high-moisture/ash-content fuels were considered the proposed process becomes unfeasible. Finally, by considering that only energy from renewable sources (such as photovoltaic panels or wind turbines) was fed to the EC, it was assessed the capability of the proposed process to be used as an energy storage system. An electric energy storage efficiency of 13% was evaluated for the system, notwithstanding the fuel considered.

Nomenclature

c_p – specific heat capacity [Jmol^{-1}K^{-1}]
h – axial co-ordinate [m]
n_i – mole of *i*-specie [mol]
$\dot{n}_i$ – molar flow-rate [mols^{-1}]
Q – thermal power [kW]
$\dot{Q}$ – volumetric flow-rate [Nm^{3}h^{-1}]
r_i – reaction rate [mols^{-1}]
R – gas universal constant, [Jmol^{-1}K^{-1}]
S – cross-section of the fuel reactor [m^2]
T – temperature [K]
W_i – solid inventory in FR [kg]
y_i – gaseous molar fraction [–]

Greek letters

$\alpha_{i,j}$ – stoichiometric coefficient
$\Delta H_{r,j}$ – standard enthalpy of reaction [Jmol^{-1}]

Subscripts or superscripts

° – standard state
AR – air reactor
Ash – ash
FB – freeboard
FR – fuel reactor
gas – gas
in – incoming
out – outcoming

Acronyms

CLC – chemical looping combustion
CLOU – Cl with oxygen uncoupling
EC – electrolysis cells array
FR – fuel reactor
OC – oxygen carrier

References

[1] Gotz, M., *et al.*, Renewable Power-to-Gas: A Technological and Economic Review, *Renew. Energ.*, *85* (2016), Jan., pp. 1371-1390
[2] Leung, D. Y. C., *et al.*, An Overview of Current Status of Carbon Dioxide Capture and Storage Technologies, *Renew. Sust. Energ. Rev.*, *39* (2014), Nov., pp. 426-443
[3] Selmam, O. S., *et al*., Public Perception of Carbon Capture and Storage (CCS): A Review, *Renew Sust Energ Rev*, *38* (2014), Oct., pp.848-863
[4] Diglio, G., *et al*., Techno-Economic Evaluation of a Small-Scale Power Generation Unit Based on a Chemical Looping Combustion Process in Fixed Bed Reactor Network, *Ind. Eng. Chem. Res*, *57* (2018), July, pp.11299-11311
[5] Diglio, G., *et al.*, Numerical Simulation of Hydrogen Production by Chemical Looping Reforming in a Dual Fluidized Bed Reactor, *Powder Technol*., *316* (2017), July, pp. 614-627
[6] Ryden, M., *et al.* , CaMn 0.875 Ti0.125O3 as Oxygen Carrier for Chemical-Looping Combustion With Oxygen Uncoupling (CLOU)—Experiments in a Continuously Operating Fluidized-Bed Reactor System, *Int. J. Greenh. Gas Control.*, *5* (2011), 2, pp. 356-366

[7] Coppola, A., *et al*., Mathematical Modeling of a Two-Stage Fuel Reactor for Chemical Looping Combustion With Oxygen Uncoupling of Solid Fuels, *Appl. Energy*, *157* (2015), Nov., pp. 449-461
[8] Ferrero, D., *et al*., A Comparative Assessment on Hydrogen Production from Low- and High-Temperature Electrolysis, *Int. J. Hydrog. Energy*, *38* (2013), 9, pp. 3523-3536
[9] Ronsch, S., *et al.*, Review on Methanation - From Fundamentals to Current Projects, *Fuel*, *9* (2015), Feb., pp. 82-102
[10] Kopyscinski, J., *et al.*, Production of Synthetic Natural Gas (SNG) From Coal and Dry Biomass – A Technology Review From 1950 to 2009, *Fuel*, *89* (2010), 8, pp.1763-1783
[11] Solsvik, J., *et al.*, Implementation of Chemical Reaction Equilibrium by Gibbs and Helmholtz Energies in Tubular Reactor Models: Application to the Steam–Methane Reforming Process, *Chem. Eng. Sci*., *140* (2017), Feb., pp 261-278
[12] Diglio, G., *et al.*, Novel Quasi-Autothermal Hydrogen Production Process in a Fixed-Bed Using a Chemical Looping Approach: A Numerical Study, *Int. J. Hydrog. Energy*, *42* (2017), 22, pp. 15010-15023
[13] ***, NIST Chemistry WebBook - SRD 69, https://dx.doi.org/10.18434/T4D303
[14] Perry, R. H., Green, D. W., *Perry's Chemical Engineers' Handbook*, McGraw-Hill, New York, USA, 2008
[15] Diglio, G., *et al.*, Numerical Assessment of the Effects of Carbon Deposition and Oxidation on Chemical Looping Combustion in a Packed-Bed Reactor, *Chem. Eng. Sci*., *160* (2017), Mar., pp 85-95
[16] Diglio, G., *et al*., Feasibility of CaO/CuO/NiO Sorption-Enhanced Steam Methane Reforming Integrated With Solid-Oxide Fuel Cell for Near-Zero-CO_2 Emissions Cogeneration System, *Appl. Energy*, *230* (2018), Nov., pp. 241-256

Paper submitted: March 23, 2020
Paper revised: May 5, 2020
Paper accepted: June 16, 2020